

The Energy Function and Cosmic Formation Rate of Fast Radio Bursts

CAN-MIN DENG,^{1,2,*} JUN-JIE WEI,^{1,†} AND XUE-FENG WU^{1,2,‡}

¹*Purple Mountain Observatory, Chinese Academy of Sciences, Nanjing 210008, China*

²*School of Astronomy and Space Science, University of Science and Technology of China, Hefei, Anhui 230026, China*

ABSTRACT

Fast radio bursts (FRBs) are intense radio transients whose physical origin remains unknown. Therefore, it is of crucial importance to use a model-independent method to obtain the energy function and cosmic formation rate directly from the observational data. Based on a sample of 28 Parkes FRBs, we determine, for the first time, the energy function and formation rate of FRBs by using the Lynden-Bell C^- method. The energy function can be well described by a broken power-law function. We also derive the cosmic formation rate which is consistent with the cosmic star formation rate up to $z \sim 3$, with a local formation rate of $\rho(0) \simeq (1.8 \pm 0.3) \times 10^4 \text{ Gpc}^{-3} \text{ yr}^{-1}$. This might be a important clue for the physical origin of FRBs.

Keywords: Fast radio burst, Formation rate, Energy function

1. INTRODUCTION

Fast radio bursts (FRBs) are intense radio transients with intrinsic durations less than several milliseconds (Lorimer et al. 2007; Thornton et al. 2013; Ravi 2019). So far, more than seventy FRBs have been detected by various telescopes (Petroff et al. 2016). They are all non-repeating sources except FRB 121102 (Spitler et al. 2016) and FRB 180814 (The CHIME/FRB Collaboration et al. 2019). Their dispersion measures (DMs) are typically hundreds of pc cm^{-3} , which are much higher than the DM contribution of our Galaxy, robustly suggest that FRBs occur at cosmological distances. This is supported by the identification of the host galaxy of the repeating FRB 121102 with redshift $z \simeq 0.19$ (Chatterjee et al. 2017; Tendulkar et al. 2017).

Many models have been proposed to explain FRBs, in which compact star origins are the most popular ideas. It was suggested that FRBs can be produced by a single neutron star (NS), such as giant pulses of young pulsars (Keane et al. 2012; Cordes & Wasserman 2016), giant flares of magnetars (Lyubarsky 2014), and magnetic field shedding of collapsing neutron stars (Zhang 2014; Falcke & Rezzolla 2014; Punsly & Bini 2016). Some compact binary mergers, specifically, mergers of double white dwarfs (WDs) (Kashiyama et al. 2013), of WD-NS (Gu et al. 2016; Liu 2018), of WD-black hole (BH) (Li et al. 2018), of double NSs (Totani 2013; Wang et al. 2016), NS-BH (Mingarelli et al. 2015), or of double BHs (Liu et al. 2016;

Zhang 2016), could be responsible for FRBs. Besides, there are also other novel models, such as pulsar traveling through asteroid belt (Dai et al. 2016), super-conducting strings (Cai et al. 2012), primordial black holes coalescence (Deng et al. 2018), and so on (see a comprehensive review Platts et al. (2018)). However, the nature of FRBs remains elusive, particularly their high all-sky rate and large released energy. The formation rate and energy function as well as their cosmological evolution are crucial for revealing the origin of FRBs. In this paper, we investigate the formation rate and energy function of FRBs. The errors quoted through this paper are all at 1σ confidence level.

2. SELECTION EFFECT AND COMPLETE SAMPLE

Up to date, a total of more than seventy FRBs have been detected by various radio telescopes including the Arecibo, ASKAP, CHIME, GBT, Parkes, Pushchino, and UTMOST, which are available from the FRB catalogue¹ (see Petroff et al. 2016 and references therein). Since different telescopes have different detection thresholds, here we only take into account the largest subsample observed by the Parkes containing 28 FRBs to ensure that the very different response functions of different telescopes will not be involved.

The observed DM of an FRB can be consisted of

$$\text{DM}_{\text{obs}} = \text{DM}_{\text{MW}} + \text{DM}_{\text{IGM}} + \frac{\text{DM}_{\text{host}}}{1+z}, \quad (1)$$

where DM_{MW} is the DM distribution from the Milky Way and DM_{host} is the DM contribution from both the FRB host

* dengcm@pmo.ac.cn

† jjwei@pmo.ac.cn

‡ xfwu@pmo.ac.cn

¹ <http://frbcat.org/>

galaxy and source environment in the cosmological rest frame of the FRB. Note that the DM of the FRB source environment is considered to be relatively much lower than that of the FRB host galaxy. The IGM portion of DM is related to the redshift of the source through (Ioka 2003; Inoue 2004; Deng & Zhang 2014)

$$\text{DM}_{\text{IGM}}(z) = \frac{3cH_0\Omega_b f_{\text{IGM}} f_e}{8\pi G m_p} \int_0^z \frac{H_0(1+z')}{H(z')} dz', \quad (2)$$

where Ω_b is baryon density, $f_{\text{IGM}} \sim 0.83$ is the fraction of baryons in the IGM (Fukugita et al. 1998), and $f_e \sim 7/8$ is the free electron number per baryon in the universe, which was first introduced by Deng & Zhang (2014). Adopting the latest Planck results for the Λ CDM cosmological parameters, i.e., $H_0 = 67.74 \text{ km s}^{-1} \text{ Mpc}^{-1}$, $\Omega_b = 0.0486$, $\Omega_m = 0.3089$, and $\Omega_\Lambda = 0.6911$ (Planck Collaboration et al. 2016), the redshifts of the FRBs can then be inferred from their DM_{IGM} . In order to obtain DM_{IGM} of an FRB, we have to figure out DM_{MW} and DM_{host} . The DM_{MW} values have been derived based on the Galactic electron density models of Cordes & Lazio (2002) or Yao et al. (2017), as provided in the FRB catalogue (see Petroff et al. 2016 and references therein), while the DM_{host} values are completely unknown. The observations of the host galaxy of FRB 121102 suggest that DM_{host} ($\sim 100 \text{ pc cm}^{-3}$) is not small, which is comparable to DM_{IGM} for FRB 121102 (Tendulkar et al. 2017). In any case, a fixed DM_{host} value can be used to derive a rough estimation on DM_{IGM} , and hence, a rough estimation on z , of a particular FRB. In our calculations, we take the values of DM_{host} varying from zero to 100 pc cm^{-3} , where the upper limit is set according to the current minimum DM of the Parkes FRBs, i.e., $\text{DM}_{\text{FRB 110214}} = \text{DM}_{\text{obs}} - \text{DM}_{\text{MW}} = 137.8 \text{ pc cm}^{-3}$ (?). This variation range of DM_{host} results in the uncertainties of redshifts and energies of the FRBs, as presented in Table 1 and Figure 1. One can see that these uncertainties are small except for those with low redshifts, and thus do not significantly affect our results.

With an inferred redshift z , we calculate the isotropic energy² of an FRB within the rest-frame bandwidth (ν_1, ν_2) by

$$E \simeq \frac{4\pi D_L^2}{1+z} F_\nu \int_{\nu_1/(1+z)}^{\nu_2/(1+z)} \left(\frac{\nu}{\nu_c}\right)^{-\alpha} d\nu, \quad (3)$$

where F_ν is the observed fluence density, D_L is luminosity distance, $\left(\frac{\nu}{\nu_c}\right)^{-\alpha}$ is the spectrum of FRBs, and $\nu_c = 1.352 \text{ GHz}$ is the typical central frequency of Parkes. Shannon et al. (2018) and Macquart et al. (2018) found

² In this paper, we care more about the observed energy rather than about the observed luminosity. That is because we note that the intrinsic pulse widths of most FRBs are unknown (Ravi 2019) and the observed energy is more physical than the observed luminosity.

that the FRB population have a mean spectrum index $\alpha = 1.8 \pm 0.3$ and $\alpha = 1.6_{-0.3}^{+0.2}$, respectively. We adopt $\alpha = 1.6$ in this paper. We take $\nu_1 = 1 \text{ GHz}$ and $\nu_2 = 8 \text{ GHz}$, because an FRB at redshift ~ 4 with characteristic frequency $\sim 8 \text{ GHz}$ can be detected in the observed band of Parkes.

As discussed by Keane & Petroff (2015), the fluence completeness should be considered when one attempts to determine the population estimates for FRBs. The detection criteria is decided by the signal-to-noise ratio (Caleb et al. 2016),

$$S/N = \frac{\beta G \sqrt{BN_p}}{T_{\text{sys}}} S_\nu \sqrt{t_{\text{obs}}}, \quad (4)$$

where β is the digitisation factor, G is the system gain in K Jy^{-1} , B is the bandwidth in MHz, N_p is the number of polarizations, T_{sys} is the system temperature in K, S_ν is the flux density of the signal in Jy, and t_{obs} is the observed pulse width in seconds. The signal is claimed as a reliable FRB detection when the S/N reaches over 10. Based on Eq (4), then we have the detection threshold in fluence density,

$$F_{\nu, \text{th}} = \frac{T_{\text{sys}}}{\beta G \sqrt{BN_p}} (S/N) \sqrt{t_{\text{obs}}}. \quad (5)$$

One can see that the detection threshold is depend on the pulse width t_{obs} . For the same F_ν , a signal with larger t_{obs} is more difficult to be detected by the telescope. If FRBs exist arbitrarily large pulse width, we are always incomplete to wide bursts because Parkes is sensitive for searching FRBs only for $t_{\text{obs}} \lesssim 32 \text{ ms}$ (Keane & Petroff 2015). Figure 2 shows the FRB sample of Parkes in the $F_\nu - t_{\text{obs}}$ plane. As shown, the maximum pulse width is 20 ms (FRB 180923) which had not reached the sensitive limit of Parkes. On the other hand, theoretically, FRBs are likely to origin from compact objects with milliseconds time-scale (Keane 2018). Therefore, we do not suffer from the width incompleteness if FRBs are the cases. According to Eq (5), we only have fluence completeness for $F_\nu \gtrsim 2 \text{ Jy ms}$ with maximum width of 32 ms, which is shown in Figure 2.

We adopt a fluence threshold limit $F_{\nu, \text{th}} \simeq 2 \text{ Jy ms}$, and pick a sub-sample containing 17 FRBs out of the Parkes sample of 28 FRBs. We define it as a complete sample³, which is a sample with a well defined truncation due to the observational selection biases. In the $E - z$ plane, the truncated threshold $F_{\nu, \text{th}} \simeq 2 \text{ Jy ms}$ is displayed by the solid line (red) in Figure 1, and the corresponding energy threshold is calculated by Eq (3). One can see that the data points show a strong concentration toward the truncation line, and 17 out

³ We note that the maximum DM detected so far is 2596 pc cm^{-3} , which is much smaller than the searching limit of Parkes (Petroff et al. 2014). Therefore, we are complete in DMs, and thus we are also complete in redshifts because the redshifts are inferred from DMs.

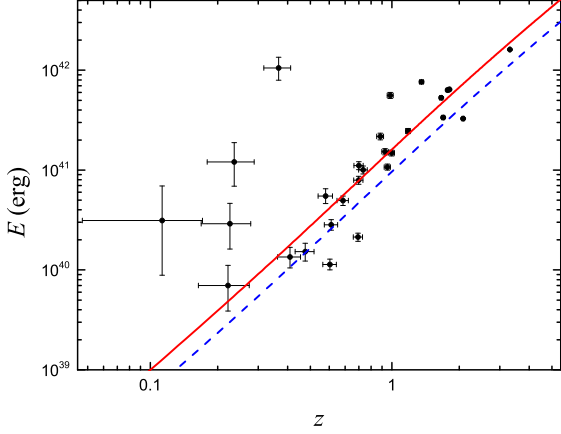


Figure 1. The energy–redshift distribution of 28 Parkes FRBs. The errors of the data correspond to the variation range of DM_{host} from zero to 100 pc cm^{-3} and the central values are given for $DM_{\text{host}} = 50 \text{ pc cm}^{-3}$. The solid line shows the threshold of $F_{\nu,\text{th}} = 2 \text{ Jy ms}$ selecting a complete sample. The dash line shows the threshold of $F_{\nu,\text{th}} = 1.2 \text{ Jy ms}$.

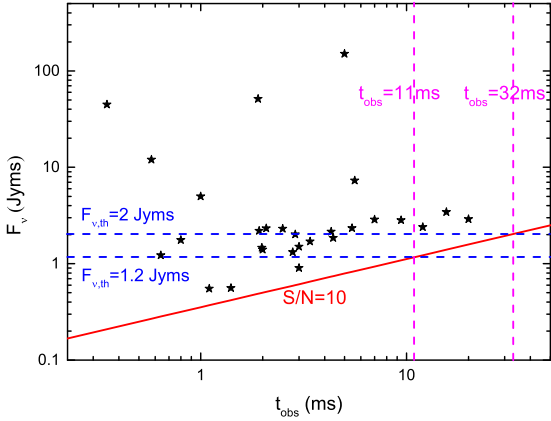


Figure 2. The fluence density–pulse width distribution of 28 Parkes FRBs (pentagrams). The solid line corresponds to the constant $S/N = 10$, above which events are detectable. Dash lines of constants t_{obs} (blue) and $F_{\nu,\text{th}}$ (purple) are also shown.

of 28 points are above the line. In the next section, we estimate the energy function and cosmic formation rate of FRBs based on this complete sample.

3. ENERGY FUNCTION AND FORMATION RATE

For a survey of a telescope, the number of FRBs detectable above its threshold limit in the redshift range (z_1, z_2) and energy range (E_1, E_2) can be expressed as

$$N = \frac{\Omega T}{4\pi} \int_{z_1}^{z_2} dz \int_{\max(E_1, E_{\min})}^{E_2} \frac{\Psi(E, z) dV}{1+z} \frac{dE}{dz}, \quad (6)$$

Here Ω and T are the field-of-view and the total observing time, respectively. dV is the co-moving volume element of the universe. E_{\min} is the minimum observable energy at z . If $\Psi(E, z)$ is known, one can calculate the observed number of FRBs by a given telescope according to Equation (6). If E is independent of z , without loss of generality, $\Psi(E, z)$ can be expanded into a degenerate (separate) form $\psi(E)\rho(z)$, where $\psi(E)$ is the energy function and $\rho(z)$ is the formation rate of FRBs.

However, as shown in Figure 1, E and z are highly correlated with each other. Of course, this might be a result of the truncated effect and would not reflect the real physics. Thus, the first step is to test the intrinsic correlation between E and z . In order to achieve the goal, we use the Efron-Petrosian method (Efron & Petrosian 1992). For the i th FRB in our sample, described by (E_i, z_i) , we can define the associated set as

$$A_i = \{j | E_j \geq E_i, z_j \leq z_{\max,i}\}, \quad (7)$$

where $z_{\max,i}$ is the maximum redshift at which the FRB with energy E_i can be detected by the telescope above the detection threshold. The number of FRBs in this associated set A_i is denoted as N_i . We further define A_i 's largest un-truncated subset as

$$B_i = \{j \in A_i | z_j \leq z_i\}. \quad (8)$$

The number of FRBs in B_i is denoted as R_i . Then we calculate the modified Kendall correlation coefficient through the statistic τ :

$$\tau = \frac{\sum_i (R_i - X_i)}{\sqrt{\sum_i V_i}}, \quad (9)$$

where $X_i = (N_i + 1)/2$ and $V_i = (N_i^2 - 1)/12$ are the expectation and variance for the uniformly scattering distribution, respectively. Theoretically, a small τ value (≈ 0) implies energy and redshift are independent, and $\tau > 1$ implies a strong dependence. We find $|\tau| \approx 0.4$ which implies that the independence between E and z is acceptable.

Since E is independent with z , we can derive the energy function $\psi(E)$ and formation rate $\rho(z)$ of FRBs respectively by applying the C^- method proposed by Lynden-Bell (1971). This method has been widely used in gamma-ray bursts (GRBs) (Lloyd-Ronning & Ramirez-Ruiz 2002; Yonetoku et al. 2004, 2014; Petrosian et al. 2015; Yu et al. 2015; Deng et al. 2016; Zhang & Wang 2018). The robustness of this method has been confirmed by these works through Monte Carlo simulations. Pescalli et al. (2016) further found that the C^- method can give more reliable results when applying to complete samples.

The cumulative energy distribution $\Phi(> E)$ can be calculated point-by-point starting from the lowest observed energy (Lynden-Bell 1971),

$$\Phi(> E_i) = \prod_{j < i} \left(1 - \frac{1}{N_j}\right), \quad (10)$$

Table 1. The observational properties and the estimated redshifts (z) and isotropic energies (E) of Parkes FRBs

| FRB Name | DM _{obs} (pc cm ⁻³) | DM _{MW} (pc cm ⁻³) | z^a | F_ν (Jy ms) | t_{obs} (ms) | E^a (10 ⁴⁰ erg) |
|-----------|---|--|--|--------------------|--------------------------|--|
| FRB010125 | 790 ± 3 | 110 | 0.73 ^{+0.03} _{-0.03} | 0.3 | 9.4 | 11.08 ^{+1.06} _{-1.01} |
| FRB010621 | 745 ± 10 | 523 | 0.21 ^{+0.05} _{-0.05} | 0.41 | 7 | 2.91 ^{+1.73} _{-1.29} |
| FRB010724 | 375 | 44.58 | 0.34 ^{+0.04} _{-0.04} | 30 | 5 | 105.04 ^{+29.58} _{-25.46} |
| FRB090625 | 899.55 ± 0.01 | 31.69 | 0.94 ^{+0.03} _{-0.03} | 1.14 | 1.92 | 15.28 ^{+1.13} _{-1.08} |
| FRB110214 | 168.9 ± 0.5 | 31.1 | 0.11 ^{+0.05} _{-0.06} | 51.3 | 1.9 | 3.13 ^{+3.80} _{-2.24} |
| FRB110220 | 944.38 ± 0.05 | 34.77 | 0.98 ^{+0.03} _{-0.03} | 7.28 | 5.6 | 55.87 ^{+3.95} _{-3.80} |
| FRB110626 | 723 ± 0.3 | 47.46 | 0.72 ^{+0.03} _{-0.03} | 0.56 | 1.4 | 2.13 ^{+0.21} _{-0.20} |
| FRB110703 | 1103.6 ± 0.7 | 32.33 | 1.17 ^{+0.03} _{-0.03} | 2.15 | 4.3 | 24.63 ^{+1.44} _{-1.40} |
| FRB120127 | 553.3 ± 0.3 | 31.82 | 0.55 ^{+0.03} _{-0.04} | 0.55 | 1.1 | 1.14 ^{+0.15} _{-0.14} |
| FRB121002 | 1629.18 ± 0.02 | 74.27 | 1.73 ^{+0.02} _{-0.02} | 2.3392 | 5.44 | 64.05 ^{+1.64} _{-1.62} |
| FRB130626 | 952.4 ± 0.1 | 66.87 | 0.96 ^{+0.03} _{-0.03} | 1.4652 | 1.98 | 10.73 ^{+0.78} _{-0.75} |
| FRB130628 | 469.88 ± 0.01 | 52.58 | 0.44 ^{+0.04} _{-0.04} | 1.2224 | 0.64 | 1.52 ^{+0.33} _{-0.29} |
| FRB130729 | 861 ± 2 | 31 | 0.90 ^{+0.03} _{-0.03} | 3.4342 | 15.61 | 21.72 ^{+1.68} _{-1.61} |
| FRB131104 | 779 ± 1 | 71.1 | 0.76 ^{+0.03} _{-0.03} | 2.3296 | 2.08 | 10.03 ^{+0.92} _{-0.88} |
| FRB140514 | 562.7 ± 0.6 | 34.9 | 0.56 ^{+0.03} _{-0.04} | 1.3188 | 2.8 | 2.84 ^{+0.36} _{-0.33} |
| FRB150215 | 1105.6 ± 0.8 | 427.2 | 0.73 ^{+0.03} _{-0.03} | 2.016 | 2.88 | 7.92 ^{+0.76} _{-0.72} |
| FRB150418 | 776.2 ± 0.5 | 188.5 | 0.63 ^{+0.03} _{-0.03} | 1.76 | 0.8 | 4.95 ^{+0.55} _{-0.52} |
| FRB150610 | 1593.9 ± 0.6 | 122 | 1.63 ^{+0.02} _{-0.02} | 1.4 | 2 | 33.62 ^{+0.92} _{-0.90} |
| FRB150807 | 266.5 ± 0.1 | 36.9 | 0.22 ^{+0.05} _{-0.05} | 44.8 | 0.35 | 12.04 ^{+6.80} _{-5.14} |
| FRB151206 | 1909.8 ± 0.6 | 160 | 1.97 ^{+0.02} _{-0.02} | 0.9 | 3 | 32.75 ^{+0.73} _{-0.72} |
| FRB151230 | 960.4 ± 0.5 | 38 | 1.00 ^{+0.03} _{-0.03} | 1.848 | 4.4 | 14.85 ^{+1.03} _{-0.99} |
| FRB160102 | 2596.1 ± 0.3 | 13 | 3.08 ^{+0.02} _{-0.02} | 1.7 | 3.4 | 160.82 ^{+2.20} _{-2.18} |
| FRB171209 | 1458 | 13 | 1.60 ^{+0.02} _{-0.02} | 2.3 | 2.5 | 53.01 ^{+1.48} _{-1.46} |
| FRB180301 | 520 | 155 | 0.38 ^{+0.04} _{-0.04} | 1.5 | 3 | 1.35 ^{+0.34} _{-0.30} |
| FRB180309 | 263.47 | 44.69 | 0.21 ^{+0.05} _{-0.05} | 11.9808 | 0.576 | 0.70 ^{+0.41} _{-0.31} |
| FRB180311 | 1575.6 | 45.2 | 1.70 ^{+0.02} _{-0.02} | 2.4 | 12 | 63.23 ^{+1.65} _{-1.63} |
| FRB180714 | 1469.873 | 257 | 1.33 ^{+0.02} _{-0.02} | 5 | 1 | 76.37 ^{+2.59} _{-2.55} |
| FRB180923 | 548 ± 3 | 46.6 | 0.53 ^{+0.04} _{-0.04} | 2.9 | 20 | 5.51 ^{+0.99} _{-0.90} |

^aThe errors of z and E correspond to the variation range of DM_{host} from 0 to 100 pc cm⁻³ and the central values are given by DM_{host} = 50 pc cm⁻³.

where $j < i$ implies that the j th FRB has a larger energy than the i th one. The normalized cumulative energy distribution $\Phi(> E)$ is shown in Figure 3, which can be well fitted by a broken power-law function. The differential energy function $\psi(E)$ can then be obtained by derivation of $\Phi(> E)$, yielding

$$\psi(E) \propto \begin{cases} E^{-1.3 \pm 0.1}, & E < E_b \\ E^{-2.4 \pm 0.1}, & E > E_b \end{cases}, \quad (11)$$

where $E_b = (3.7 \pm 0.7) \times 10^{40}$ erg is the break energy.

To derive the cosmic formation rate $\rho(z)$ of FRBs, we define another associated set C_i as,

$$C_i = \{j | z_j < z_i, E_j \geq E_i^{\min}\}, \quad (12)$$

where z_i is the redshift of i th FRB and $E_{0,i}^{\min}$ is the minimum observable energy at redshift z_i . The number of FRBs in C_i is denoted as M_i . Similar to deriving the energy function,

we can obtain the cumulative redshift distribution $\phi(< z)$ as (Lynden-Bell 1971),

$$\phi(< z_i) = \prod_{j < i} \left(1 + \frac{1}{M_j}\right). \quad (13)$$

We can derive the FRB cosmic formation rate $\rho(z)$ with the following formula,

$$\rho(z) \propto (1+z) \frac{d\phi(< z)}{dz} \left(\frac{dV}{dz}\right)^{-1}, \quad (14)$$

where the factor $(1+z)$ comes from the cosmological time dilation. Figure 4 gives the formation rate of FRBs (blue step line) comparing with the cosmic star formation rate (gray points). One can see that normalized cosmic formation of FRBs is roughly consistent with the cosmic star formation rate (SFR) out to $z \sim 1.7$. Moreover, one can obtain the local

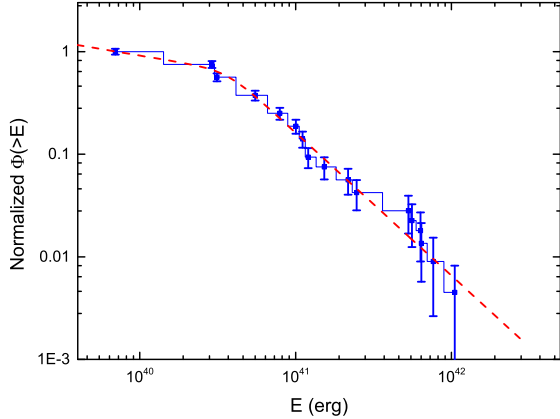


Figure 3. The normalized cumulative energy distribution of FRBs. The uncertainties are the Poisson uncertainties of N_j . The dash line is the best fit to the data with $\chi^2/dof = 0.9$.

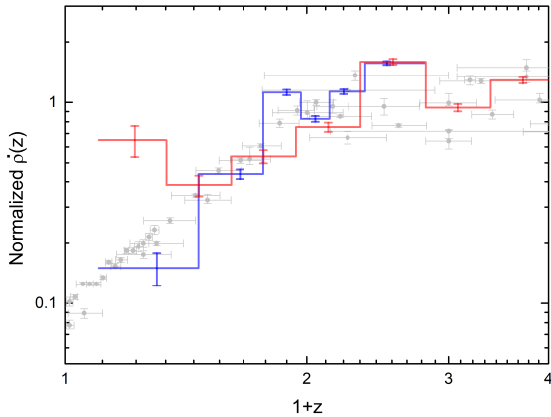


Figure 4. The normalized cosmic formation rate $\rho(z)$ of FRBs (step lines), the error bars are obtained from the Poisson uncertainties of M_j . The blue step line is derived by the complete sample (17 FRBs). The red step line is derived by the slightly incomplete sample (25 FRBs). The cosmic star formation rate (gray points) obtained from Hopkins & Beacom (2006) is also shown for comparison.

formation rate $\rho(0) \simeq 1.8 \pm 0.3 \times 10^4 \text{ Gpc}^{-3}\text{yr}^{-1}$ by adopting the field-of-view and observing time per burst for searching FRBs of Parkes as $144.1 \text{ deg}^2 \text{ h}$ (Champion et al. 2016) and assuming no beaming effect. Cao et al. (2018) also obtained the similar local rate, several times $10^4 \text{ Gpc}^{-3}\text{yr}^{-1}$, by assuming FRBs are associated with mergers of compact binary stars. However, it is worth pointing out that our result is directly obtained from the data and has no model assumptions.

Due to the conservative detection threshold setting, the complete sample only contains 17 FRBs and lacks of high z sources. In order to contain more sources into the analysis, especially the high z sources, we further adopt a lower thresh-

old $F_{\nu, \text{th}} \simeq 1.2 \text{ Jyms}$ which contains 25 FRBs. However, as shown in Figure 2, this threshold selects a complete sample only for pulse width $t_{\text{obs}} \lesssim 11 \text{ ms}$, and three bursts have width larger than 11 ms. Therefore, this sample is somewhat incomplete. Even so, based on this sample, we estimate the cosmic formation rate of FRBs. The results are shown in Figure 4 (red step line) comparing with the cosmic star formation rate. One can see that the normalized cosmic formation rate of FRBs is consistent with the cosmic star formation rate out to $z \sim 3$, except for the first point at lowest z . However, the excess of the first point is believed to be caused by the incompleteness of the sample as discussed in Pescalli et al. (2016).

By combining the the results of the complete sample (17 FRBs) and the incomplete sample (25 FRBs), we find that the cosmic formation rate of FRBs is consistent with the cosmic star formation rate out to $z \sim 3$.

4. CONCLUSION AND DISCUSSION

In this work, we use the Lynden-Bell C^- method to study the released energy function and cosmic formation rate of FRBs without model assumptions. This is the first time for applying this method to FRBs. Firstly, we find that the energy of FRBs is independent of the redshift. We derive the differential energy function, which can be well fitted with a broken power-law as $\psi(E) \propto E^{-1.3 \pm 0.1}$ for $E < E_b$ and $\psi(E) \propto E^{-2.4 \pm 0.1}$ for $E > E_b$, where $E_b = (3.7 \pm 0.7) \times 10^{40} \text{ erg}$ is the break energy. Moreover, we also derive the cosmic formation rate of FRBs. It is a surprise that the normalized cosmic formation rate of FRBs is well consistent with the cosmic star formation rate up to $z \sim 3$, with a local rate of $\rho(0) \simeq (1.8 \pm 0.3) \times 10^4 \text{ Gpc}^{-3}\text{yr}^{-1}$.

Since we have not yet known the physical origin of FRBs, it is of crucial importance to use the non-parametric method to obtain the energy function and formation rate directly from the data, which can help us understand the nature of FRBs. In this paper, we find that the cosmic formation rate of FRBs is well consistent with the cosmic star formation rate up to $z \sim 3$. Our results suggest the formation of FRBs might connect to the death of massive stars, or the remains of their death. Moreover, the type II+Ib/c supernova rate is expected to be $10^{-3} \sim 10^{-2} \text{ yr}^{-1}$ per galaxy (Cappellaro et al. 1999), which corresponds to a local rate $10^4 \sim 10^5 \text{ Gpc}^{-3}\text{yr}^{-1}$. This is roughly consistent with the local rate of FRBs. Interestingly, right after our first submission, we note that Locatelli et al. (2018) found, for the Parkes sample, the cosmic formation rate of FRBs is consistent with cosmic star formation rate by performing the luminosity-volume test.

Recently, the CHIME telescope found 13 new FRBs during the pre-commissioning phase (The CHIME/FRB Collaboration et al. 2019; CHIME/FRB Collaboration et al. 2019). They expected CHIME can detect 2–42 FRBs per day (CHIME/FRB Collaboration

2018). If so, thousands of FRBs over 3 years lifetime of the project will be detected. We can re-study this subject more intense by using a much larger sample by that time.

5. ACKNOWLEDGMENTS

We thank S.-B. Zhang for helpful discussion. This work is partially supported by the National Natural Science Foundation of China (grant Nos. 11603076, 11673068, 11725314,

and U1831122), the Youth Innovation Promotion Association (2017366), the Key Research Program of Frontier Sciences (QYZDB-SSW-SYS005), the Strategic Priority Research Program “Multi-waveband gravitational wave Universe” (grant No. XDB23000000) of the Chinese Academy of Sciences, and the “333 Project” and the Natural Science Foundation (Grant No. BK20161096) of Jiangsu Province.

REFERENCES

- Cai, Y.-F., Sabancilar, E., & Vachaspati, T. 2012, *PhRvD*, 85, 023530
- Caleb, M., Flynn, C., Bailes, M., et al. 2016, *MNRAS*, 458, 708
- Cao, X.-F., Yu, Y.-W., & Zhou, X. 2018, *ApJ*, 858, 89
- Cappellaro, E., Evans, R., & Turatto, M. 1999, *A&A*, 351, 459
- Champion, D. J., Petroff, E., Kramer, M., et al. 2016, *MNRAS*, 460, L30
- Chatterjee, S., Law, C. J., Wharton, R. S., et al. 2017, *Nature*, 541, 58
- CHIME/FRB Collaboration, Amiri, M., Bandura, K., et al. 2018, *ApJ*, 863, 48
- The CHIME/FRB Collaboration, :, Amiri, M., et al. 20191, arXiv:1901.04525
- CHIME/FRB Collaboration, :, Amiri, M., et al. 2019, arXiv:1901.04524
- Cordes, J. M., & Lazio, T. J. W. 2002, arXiv:astro-ph/0207156
- Cordes, J. M., & Wasserman, I. 2016, *MNRAS*, 457, 232
- Dai, Z. G., Wang, J. S., Wu, X. F., & Huang, Y. F. 2016, *ApJ*, 829, 27
- Deng, C.-M., Wang, X.-G., Guo, B.-B., et al. 2016, *ApJ*, 820, 66
- Deng, C.-M., Cai, Y., Wu, X.-F., & Liang, E.-W. 2018, *PhRvD*, 98, 123016
- Deng, W., & Zhang, B. 2014, *ApJL*, 783, L35
- Efron, B., & Petrosian, V. 1992, *ApJ*, 399, 345
- Falcke, H., & Rezzolla, L. 2014, *A&A*, 562, A137
- Fukugita, M., Hogan, C. J., & Peebles, P. J. E. 1998, *ApJ*, 503, 518
- Gu, W.-M., Dong, Y.-Z., Liu, T., Ma, R., & Wang, J. 2016, *ApJL*, 823, L28
- Hopkins, A. M., & Beacom, J. F. 2006, *ApJ*, 651, 142
- Inoue, S. 2004, *MNRAS*, 348, 999
- Ioka, K. 2003, *ApJL*, 598, L79
- Kashiyama, K., Ioka, K., & Mészáros, P. 2013, *ApJL*, 776, L39
- Keane, E. F., Stappers, B. W., Kramer, M., & Lyne, A. G. 2012, *MNRAS*, 425, L71
- Keane, E. F., & Petroff, E. 2015, *MNRAS*, 447, 2852
- Keane, E. F. 2018, *Nature Astronomy*, 2, 865
- Li, L.-B., Huang, Y.-F., Geng, J.-J., & Li, B. 2018, *Research in Astronomy and Astrophysics*, 18, 061
- Liu, X. 2018, *Ap&SS*, 363, 242
- Liu, T., Romero, G. E., Liu, M.-L., & Li, A. 2016, *ApJ*, 826, 82
- Lloyd-Ronning, N. M., & Ramirez-Ruiz, E. 2002, *ApJ*, 576, 101
- Locatelli, N., Ronchi, M., Ghirlanda, G., & Ghisellini, G. 2018, arXiv:1811.10641
- Lorimer, D. R., Bailes, M., McLaughlin, M. A., Narkevic, D. J., & Crawford, F. 2007, *Science*, 318, 777
- Lynden-Bell, D. 1971, *MNRAS*, 155, 95
- Lyubarsky, Y. 2014, *MNRAS*, 442, L9
- Macquart, J.-P., Shannon, R. M., Bannister, K. W., et al. 2018, arXiv:1810.04353
- Mingarelli, C. M. F., Levin, J., & Lazio, T. J. W. 2015, *ApJL*, 814, L20
- Pescalli, A., Ghirlanda, G., Salvaterra, R., et al. 2016, *A&A*, 587, A40
- Petroff, E., van Straten, W., Johnston, S., et al. 2014, *ApJL*, 789, L26
- Petroff, E., Barr, E. D., Jameson, A., et al. 2016, *PASA*, 33, e045
- Petroff E., Oostrum L. C., Stappers B. W., et al., 2019, *MNRAS*, 482, 3109
- Petrosian, V., Kitanidis, E., & Kocevski, D. 2015, *ApJ*, 806, 44
- Platts, E., Weltman, A., Walters, A., et al. 2018, arXiv:1810.05836
- Planck Collaboration, Ade, P. A. R., Aghanim, N., et al. 2016, *A&A*, 594, A13
- Punsly, B., & Bini, D. 2016, *MNRAS*, 459, L41
- Ravi, V. 2019, *MNRAS*, 482, 1966
- Shannon, R. M., Macquart, J.-P., Bannister, K. W., et al. 2018, *Nature*, 562, 386
- Spitler, L. G., Scholz, P., Hessels, J. W. T., et al. 2016, *Nature*, 531, 202
- Tendulkar, S. P., Bassa, C. G., Cordes, J. M., et al. 2017, *ApJL*, 834, L7
- Thornton, D., Stappers, B., Bailes, M., et al. 2013, *Science*, 341, 53
- Totani, T. 2013, *PASJ*, 65, L12
- Wang, J.-S., Yang, Y.-P., Wu, X.-F., Dai, Z.-G., & Wang, F.-Y. 2016, *ApJL*, 822, L7
- Yao, J. M., Manchester, R. N., & Wang, N. 2017, *ApJ*, 835, 29
- Yonetoku, D., Murakami, T., Nakamura, T., et al. 2004, *ApJ*, 609, 935

Yonetoku, D., Nakamura, T., Sawano, T., Takahashi, K., &
Toyanago, A. 2014, ApJ, 789, 65
Yu, H., Wang, F. Y., Dai, Z. G., & Cheng, K. S. 2015, ApJS, 218,
13

Zhang, B. 2014, ApJL, 780, L21
Zhang, B. 2016, ApJL, 827, L31
Zhang, G. Q., & Wang, F. Y. 2018, ApJ, 852, 1